EPSC2018

SB19/OPS12/EXO6 abstracts

13 Sep 2018 15:37:41

EPSC Abstracts
Vol. 12, EPSC2018-113, 2018
European Planetary Science Congress 2018

Spin-orbit resonances around an ringed elongated body: beyond the first order

Bruno Sicardy (1)
(1) LESIA, Observatoire de Paris, Université PSL, CNRS, UPMC, Sorbonne Université, Univ. Paris Diderot, Sorbonne Paris Cité, 5 place Jules Janssen, 92195 Meudon, France

Abstract

Mean motion resonances between ring particles and a perturbing satellite have been widely studied in the case of the giant planets. Among them, the Lindblad first-order resonances cause spiral-wave patterns in the ring, with an exchange of angular momentum between the disk and the satellite. Higher-order resonances are weaker and usually cause the self-crossing of the resonant streamlines, and have been little studied for those reasons. The recent discoveries of rings around small and non-spherical bodies like Chariklo and Haumea [1, 2] have triggered new interests, as the large elongations of the bodies cause strong resonances between the spin of the body and the mean motion of the ring particles, including higher-order resonances. Here we focus on the second order 2/4 and fourth order 2/6 resonances that are relevant for Chariklo and Haumea. The topologies of the phase portaits for those resonances are such that the 1/2 has a strong effect on ring particles, while the 2/6 resonances is much weaker.

1. Introduction

Both ringed-objects Chariklo and Haumea have shapes that significantly depart for spherical [2, 3]. As such they can create tesseral-type spin-orbit resonances involving the spin rate of the body, Ω, and the mean motion of the ring particles, n. More precisely, these resonances occur for

$$j\kappa = m(n - \Omega),\ m \text{ integer} \quad (1)$$

where κ is the particle epicyclic horizontal frequency, j is a positive integer and m is positive or negative integer (corresponding to inner and outer resonances, respectively). Since $\kappa \sim n$, the relation above reads

$$\frac{n}{\Omega} \sim \frac{m}{m-j}, \quad (2)$$

referred to as a $m/(m-j)$ spin-orbit resonance. From d'Alembert's rules, the corresponding resonance term of the perturbing potential is of degree j in the particle orbital eccentricity. The case $j = 1$ corresponds to Lindblad resonances (LRs), that have been extensively studied in the context of Saturn's rings, where they cause conspicuous spiral waves.

Higher-order resonances ($j > 1$) have received little attention because (i) they require higher expansions of the hydrodynamical equation of motion in the disk, a difficult task, and (ii) they cause the self-crossing of the streamlines, thus creating shocks and invalidating the usual hydrodynamical equations due to singularities in those equations.

2. Resonances around an elongated body

We examine in more details the cases $j = 2$ and $j = 4$, and discuss their impacts on rings.

Because they are small, Chariklo and Haumea's shapes depart significantly from spherical. Haumea is highly elongated, with an ellipsoidal shape of principal semi-axes $A \times B \times C = 1161 \times 852 \times 513$ km [2]. Definining the elongation parameter as $\epsilon = (A - B)/R$, where $R = \sqrt{3}(1/A^2+1/B^2+1/C^2)^{-1/2}$, we obtain $\epsilon = 0.43$ for Haumea, and a possible $\epsilon = 0.16$ for Chariklo [3]. The non-axisymmetric terms of the potentials are then proportional to $\epsilon^{|m/2|} \cos[m(\lambda - \Omega t)]$, where λ is the mean longitude.

For symmetry reasons, m is even, the strongest resonances occuring for $m = \pm 2$. Besides the first-order LRs ($j = 1$), the outermost and strongest resonance occurs for $m = -2, j = -2$, corresponding to $n/\Omega = 2/4$. Note that altough this resonance looks like the first order 1/2 LR, it is not because of it is second-order nature.

Another resonance of interest is $m = -2, j = -4$ (fourth-order), corresponding to $n/\Omega = 2/6$, as both Chariklo and Haumea's rings appear to orbit close to that resonance [2, 3].

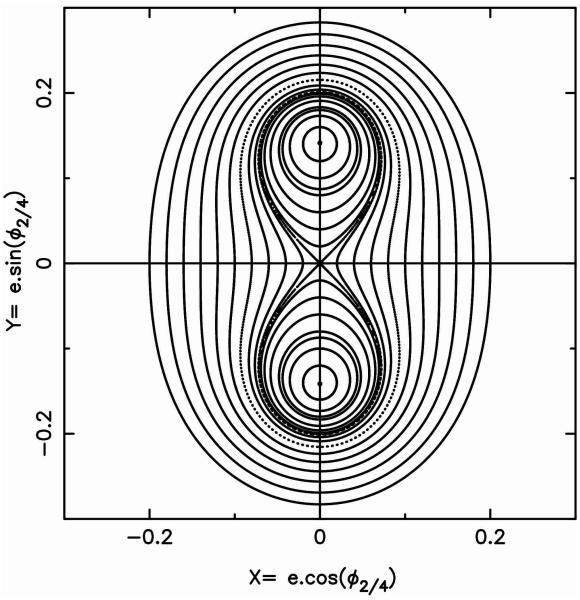

Figure 1: A typical phase portrait of the $n/\Omega = 2/4$ resonance near exact commensurability.

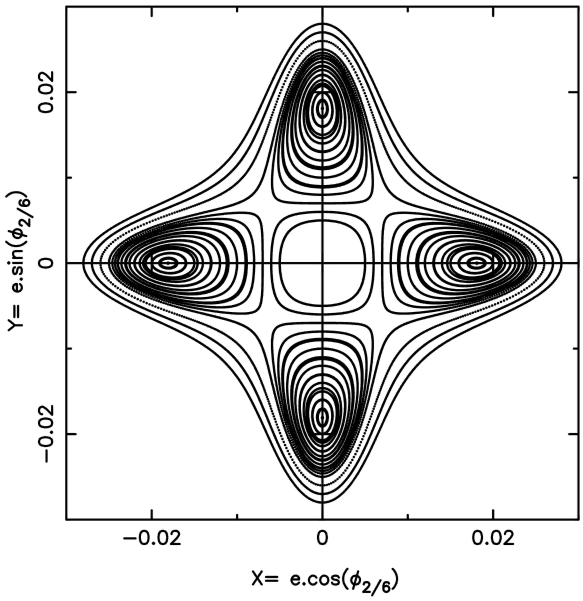

Figure 2: The same as Fig. 1 for the $n/\Omega = 2/6$ resonance.

3. Topology of the 2/4 and 2/6 resonances

Typical phase portraits of the 2/4 and 2/6 resonances are shown in Figs. 1 and 2. The relevant variables are $(X, Y) = [e \cdot \cos(\phi_{m/(m-j)}), e \cdot \sin(\phi_{m/(m-j)})]$, where the resonant angle is generically given by [4]:

$$\phi_{m/(m-j)} = \frac{m\Omega t - (m-j)\lambda - j\varpi}{j} \qquad (3)$$

A fundamental difference between the two resonances is that close to the exact resonance radius $a_{2/4}$ (more exacty in a neighborhood of width $\sim \epsilon \cdot a_{2/4}$), the 2/4 phase portrait has a hyperbolic, unstable point near the origin (Fig. 1), while near the 2/6 resonance, there is always a stable elliptic point (Fig. 2).

Collisions in dense rings tend to damp the orbital eccentricities of the particles, bringing them closer to the origin in the (X, Y) space. As a consequence, the 2/4 resonance forces the orbital eccentricity of the particles in the neighborhood $\sim \epsilon \cdot a_{2/4}$, while collisions damp the eccentricities near the 2/6 resonances, resulting in circular, mildly perturbed streamlines.

4. Summary and Conclusions

The second and fourth order spin-orbit resonances 2/4 and 2/6, respectively, between an elongated body and ring particles have structurally different phase portraits. This results in strong perturbations due to the 2/4 resonance, and much weaker perturbations from the 2/6 resonance. Applications to Chariklo and Haumea will be discussed.

Acknowledgements

The work leading to this results has received funding from the European Research Council under the European Community's H2020 2014-2020 ERC Grant Agreement No. 669416 "Lucky Star".

References

[1] Braga-Ribas, F. *et al.*: A ring system detected around the Centaur (10199) Chariklo. Nature, Vol. 508, 72-75, 2014.

[2] Ortiz, J.L. *et al.*: The size, shape, density and ring of the dwarf planet Haumea from a stellar occultation. Nature, Vol. 550, 219-223, 2017.

[3] Leiva, R. *et al.*: Size and Shape of Chariklo from Multi-epoch Stellar Occultations. Astron. J., Vol. 154, 159, 2017.

[4] Murray, C.D. and Dermott, S.F.: Solar system dynamics, Cambridge University Press, 1999.

EPSC Abstracts
Vol. 12, EPSC2018-177, 2018
European Planetary Science Congress 2018

Cassini observations of the outer edge of Saturn's A ring

Carl D. Murray and Nicholas J. Cooper
Astronomy Unit, School of Physics and Astronomy, Queen Mary University of London, UK (C.D.Murray@qmul.ac.uk)

Abstract

The outer part of Saturn's A ring between the Keeler Gap at a radius of 136,505km and the edge of the A ring at 136,770km has several resonant features, including the 33:32, 34:33 and 35:34 resonances with Prometheus. The strong 7:6 resonance with Janus can have a dominating effect on the edge of the A ring [1] especially during the four-year intervals when the Janus-Epimetheus orbital configuration places the Janus resonance close to the ring's edge [2].

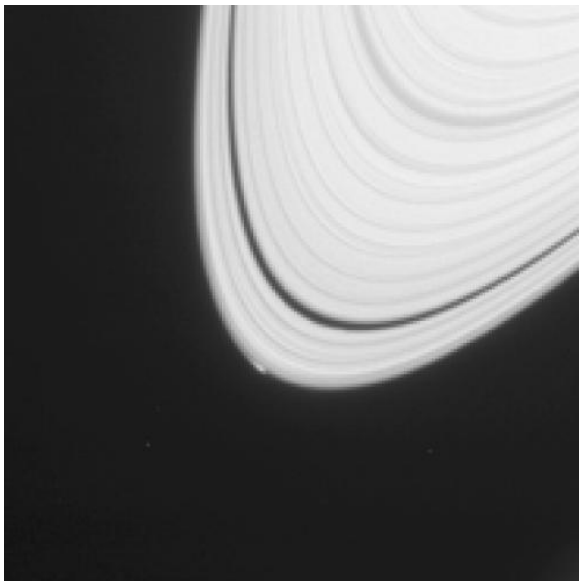

Figure 1: Object "Peggy" – a disturbance visible at the outer edge of Saturn's A ring. This is part of a Cassini ISS narrow angle camera image taken on 2013 April 15. (PIA18078. Image Credit: NASA/JPL-Caltech/Space Science Institute)

Observations of this region by the Imaging Science Subsystem (ISS) instrument onboard the Cassini spacecraft throughout the 17y duration of the mission have revealed how the various resonances affect the ring structure. In particular, the large (~13km) amplitude, radial distortions produced by the 7:6 inner Lindblad resonance with Janus dominate the A ring's structure beyond the Prometheus 35:34 inner Lindblad resonance at 136,732km.

The discovery and subsequent tracking of a feature (nicknamed "Peggy"; see Fig.1) orbiting close (within ~10km) to the A ring edge led to a more detailed examination of this entire region, especially towards the end of the mission when some of the highest resolution images were obtained. This has revealed that the semi-major axis of "Peggy" appears to have undergone a stochastic evolution of +/-5km between 2013 and 2017, probably as a result of encounters with other objects. Furthermore, the object itself appears to be embedded in a wider (+/-5°) region of material, possibly debris from a collision.

This talk will use ISS images and knowledge of resonant dynamics to characterize and review our understanding of this dynamically fascinating region.

Acknowledgements

The authors gratefully acknowledge funding from the UK Science and Technology Facilities Council through grant No. ST/P000622/1.

References

[1] Spitale, J.N. and Porco, C.C: Time variability in the outer edge of Saturn's A-ring revealed by Cassini imaging, Astron. J., 138, pp. 1520–1528, 2009.

[2] El Moutamid, M, Nicholson, P.D, French, R.G., Tiscareno, M.S., Murray, C.D., Evans, M.W., McGhee French, C., Hedman, M.M. and Burns, J.A.: How Janus' orbital swap affects the edge of Saturn's A ring?, Icarus, 279, pp. 125–140, 2016.

[3] Murray, C.D., Cooper, N.J., Williams, G.A., Attree, N.O. and Boyer, J.S.: The discovery and dynamical evolution of an object at the outer edge of Saturn's A ring, Icarus, 236, pp. 165–168, 2014.

EPSC Abstracts
Vol. 12, EPSC2018-190, 2018
European Planetary Science Congress 2018

Modeling the density profile of the outer A ring with an axisymmetric diffusion model

F. Grätz, M. Seiler, M. Seiß and F. Spahn, Institut für Physik und Astronomie, Universität Potsdam, Germany,
fgraetz@uni-potsdam.de

Abstract

1 Abstract

Numerical and theoretical studies over the last decades have shown, that bodies embedded in protoplanetary discs or planetary rings create *a)* S-shaped density modulations, dubbed propellers, if their masses do not exceed a certain threshold or *b)* cause a gap around the entire circumference of the disc if the embedded bodies mass exceeds it [1, 2]. Two counteracting physical processes govern the dynamics and determine, which structure is created: The gravitational disturber exerts a torque on nearby disc particles, sweeping them away from their original radial location, thus depleting the disc's density in its vicinity and trying to form a gap. Diffusive spreading of the disc material due to particle interactions counteracts the gravitational scattering and has the tendency to refill the gap.
At the EPSC 2017 we presented a model that describes the azimuthally averaged surface density Σ of a planetary ring in the vicinity of an embedded moon (radial gap profile) with a diffusion equation that accounts for the gravitational scattering of the ring particles as they pass the moon and for the counteracting viscous diffusion that has the tendency to fill the created gap.
In this talk we use our diffusion equation to model the density profile of the outer A ring: Resonances with the large outer moons of Saturn cause a reduction of the outwards viscous flow of the ring material at the resonance locations. The balance of viscous flow and the inward drift caused by the perturbing moons define the profile of the ring. We show, that the density profile of the outer A ring is predominantly defined and maintained by the resonances with the moons Pandora, Prometheus, Janus, Epimetheus and Mimas. Despite its vicinity to the A ring edge, Atlas has a negligible effect on the rings' density profile. Finally we compare our model to measurements performed by [3] and [4].

References

[1] Spahn, F., Sremčević, M.: Density patterns induced by small moonlets in Saturn's rings?, Astronomy and Astrophysics, Vol. 358, pp. 368-372, 2000

[2] Sremčević, M., Spahn, F., Duschl, W.: Density structures in perturbed thin cold discs, Monthly Notices of the Royal Astronomical Society, Vol. 337, pp. 1139-1152, 2002

[3] Tiscareno, M. S. and Harris, B. E.: Mapping spiral waves and other radial features in Saturn's rings, ArXiv e-prints, 1708.03702, 2017

[4] Radwan Tajeddine and Philip D. Nicholson and Pierre-Yves Longaretti and Maryame El Moutamid and Joseph A. B urns: What Confines the Rings of Saturn?, The Astrophysical Journal Supplement Series, Vol. 232, p. 28, 2017

EPSC Abstracts
Vol. 12, EPSC2018-401-1, 2018
European Planetary Science Congress 2018

Detecting rings around exoplanets

Babatunde Akinsanmi (1,2), Mahmoudreza Oshagh (1,3), Nuno Santos (1,2) and Susana Barros (1)
(1) Institute of Astrophysics and Space Science, Universidade do Porto, Portugal (tunde.akinsanmi@astro.up.pt)
(2) Departamento de Física e Astronomia, Faculdade de Ciências, Universidade do Porto (3) Institut für Astrophysik, Georg-August-Universität Göttingen, Friedrich-Hund-Platz 1, 37077 Göttingen, Germany.

Abstract

It is theoretically possible for rings to have formed around extrasolar planets in a similar way to how they formed around the giant planets in our solar system. However, no such rings have been detected to date. We test the possibility of detecting rings around exoplanets by investigating the photometric and spectroscopic transit signals of a ringed planet since they are expected to show deviations from that of a spherical planet. We develop a numerical tool (SOAP 3.0) to simulate ringed planet transits and quantify the detectability of rings based on these deviations. We found that it is possible to detect the signature of rings especially around planets with high impact parameter using time resolution ≤ 7 mins in the photometry and 15 mins in the spectroscopy. We also show that state-of-the-art instruments like CHEOPS and ESPRESSO present good prospects for detecting rings.

1. Introduction

Planetary transits offer very valuable information about planets which are not accessible through other planet detection techniques. When planets transit their host star, they obscure part of the stellar light. Photometrically, a dimming of the stellar light is observed thereby producing a light-curve. Spectroscopically, some of the radial velocity (RV) components of the rotating star is blocked causing an anomaly (line profile asymmetry) referred to as the Rossiter-McLauglin (RM) effect.

Planetary rings are unique features in our solar system yet to be detected around extrasolar planets. The rings of the Solar System giant planets have raised questions on the existence of rings around exoplanets [2][3]. The detection of exoplanetary rings could change or question our understanding of planetary formation and evolution.

1.1. SOAP 3.0 - Ringed planet transit tool

SOAP 3.0 is a numerical tool developed to simulate the transit light-curve, RM signal and the induced anomalies in these signals due to the transit of the ringed planet. The tool assumes that rings are circular, thin, opaque and extend beyond planet's radius. The ring is defined by 4 parameters: the inner and outer ring radii R_{in} and R_{out}, the ring inclination i_r with respect to sky plane and the tilt of ring plane θ with respect to orbital plane.

2. Detecting ring singnatures

Since giant close-in planets are the easiest planets to detect owing to the large transit depths and RV signal they produce, we test the scenario of detecting saturn-like rings around a close-in giant planet with parameters selected to satisfy the physical ring conditions. [3] showed that exoplanets with semi-major axis beyond 0.1 AU could host silicate rings and if optically thick, the rings would have long life time of up to 10^9 yr. Ringed planet transits produce deeper and longer transits than spherical planets but the outstanding feature induced by rings is the anomaly seen when the ring's outer edge, inner edge, and planet edge contact the stellar disc at ingress and egress phases.

The ring signature in a transit signal is the residual between the ringed planet signal and the best-fit ringless planet model [1]. Therefore, the maximum residuals indicating the ring signature is positioned around ingress and egress. Figure 1 shows the ringless model fits to the light curve and RM signal of the simulated face-on and edge-on ringed planet transits. At edge-on ($i_r, \theta = 90, 90$), the rings are not visible since they are very thin and so no ring signature is noticed in the residual. However the face-on ringed planet ($i_r, \theta = 0, 0$) produces large residuals (455 ppm for flux and 3.15 m/s for RM) at ingress and egress phases. With a photometric and RV precision of 100 ppm and 1m/s respectively, these ring signatures can be detected.

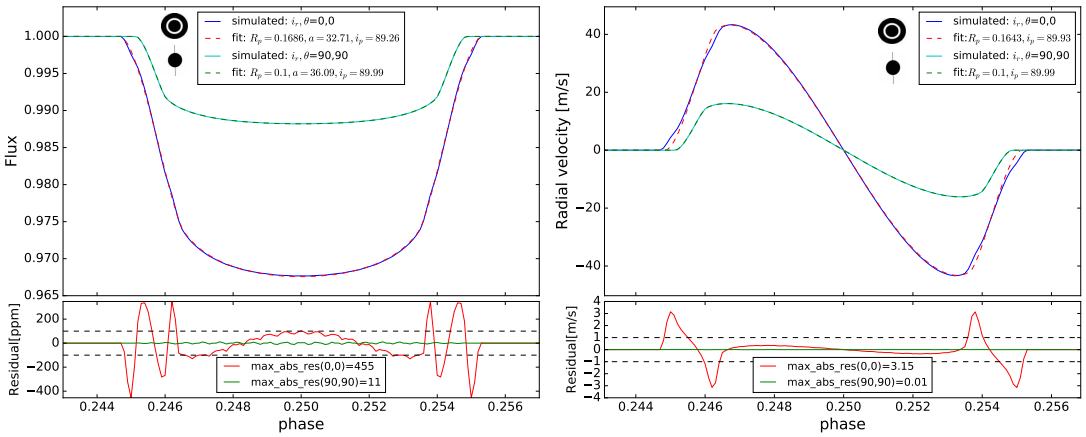

Figure 1: Ringless model fit to light-curve (left) and RM signal (right) of two ring orientations (face-on and edge-on) of the ringed planet. The black dashed line in residual plots show the detection limit of 100 ppm for photometry and 1 m/s for radial velocity. (R_p = planet radius, a = semi-major axis, i_p = orbit inclination).

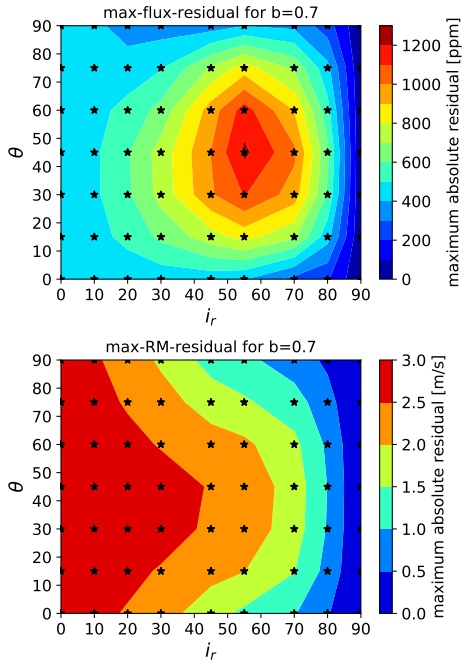

Figure 2: Contour plot from light-curve (top) and RM signal (bottom) fit residuals of 63 ring orientations.

In Fig. 2, we make contour plot of the residuals obtained from ringless fit to 63 different ring orientations of a simulated ringed planet. The red contours shows regions where ring signatures are high and easily detectable while the blue shows the low detectability regions.

3. Summary and Conclusions

We used the tool to characterise ring signatures considering different possible orientations of the ring and showed the ring orientations that are favourable for detection. We found out that high impact parameter transit can lead to large ring signatures. Also transits across fast rotating stars can lead to large spectroscopic ring signatures. We found that time resolution of $\leq$7 mins in the photometry and 15 mins in the spectoscopy is needed for ring detection. State-of-the-art instruments like CHEOPS and ESPRESSO will increase ring detectability with their better precisions.

Acknowledgements

This work was supported by Fundação para a Ciência e a Tecnologia (FCT, Portugal) through national funds and by FEDER through COMPETE2020.

References

[1] Barnes, J. W., & Fortney, J. J.: Transit Detectability of Ring Systems around Extrasolar Giant Planets, ApJ, 616, 1193. 2004.

[2] Brown, T. M., Charbonneau, D., Gilliland, R. L., Noyes, R. W., & Burrows, A.:Hubble Space Telescope Time-Series Photometry of the Transiting Planet of HD 209458, 2001.

[3] Schlichting, H. E., & Chang, P.: On the Nature of Rings around Extrasolar Planets That Reside inside the Ice Line. ApJ, 734, 117. 2011.

EPSC Abstracts
Vol. 12, EPSC2018-744, 2018
European Planetary Science Congress 2018

Analysis of Santos-Dumont's asymmetric propeller gaps

H. Hoffmann, M. Seiler, M. Seiß, and F. Spahn
Institute of Physics and Astronomy, University of Potsdam, Germany (hohoff@uni-potsdam.de)

Abstract

Among the great discoveries of the Cassini mission are the propeller-shaped structures created by small moonlets embedded in Saturn's dense rings. These moonlets are not massive enough to counteract the viscous ring diffusion to open and maintain circumferential gaps, distinguishing them from ring-moons like Pan and Daphnis.

However, *partial* gaps are one of the defining features of propeller structures. Until recently only the largest known propeller named Blériot was known to show well-formed partial gaps in images taken by the Narrow Angle Camera onboard the Cassini spacecraft. Since then, partial gaps were also resolved for the propellers Earhart and Santos-Dumont in high resolution images taken during Cassini's Ring Grazing Orbits.

We analyze images of the sunlit side of Saturn's outer A ring which show the propeller Santos-Dumont with clearly visible, azimuthally asymmetric gaps. We discuss relevant timescales for this asymmetry and interpret the azimuthal evolution in the context of a simple model of a librating moonlet [1], which links the asymmetric gaps to the reported propeller offset motion [2, 1, 3].

Acknowledgements

This work has been supported by the Deutsche Forschungsgemeinschaft (Ho 5720/1-1, Sp 384/28-2) and the Deutsches Zentrum für Luft- und Raumfahrt (OH 1401).

References

[1] Seiler, M., Sremčević, M., Seiß, M., Hoffmann, H., and Spahn, F.: A Librational Model for the Propeller Blériot in the Saturnian Ring System, ApJL, Vol. 840, L16, 2017.

[2] Tiscareno, M. S., Burns, J. A., Sremčević, M., Beurle, K., Hedman, M. M., Cooper, N. J., Milano, A. J., Evans, M. W., Porco, C. C., Spitale, J. N., and Weiss, J. W.: Physical Characteristics and Non-Keplerian Orbital Motion of "Propeller" Moons Embedded in Saturn's Rings, ApJL, Vol. 718, L92, 2010.

[3] Spahn, F., Hoffmann, H., Rein, H., Seiß, M., Sremčević, M., and Tiscareno, M. S.: Moonlets in dense planetary rings, in: Planetary Ring Systems, Eds: M. S. Tiscareno, C. D. Murray, Cambridge University Press, ISBN 9781107113824, 2018.

EPSC Abstracts
Vol. 12, EPSC2018-756, 2018
European Planetary Science Congress 2018

Hydrodynamic Simulations of Asymmetric Propeller Structures in the Saturnian Ring System

Michael Seiler, Martin Seiß, Holger Hoffmann and Frank Spahn
Institute of Physics and Astronomy, University of Potsdam, Germany (miseiler@uni-potsdam.de)

Abstract

Small sub-kilometer sized objects (called moonlets) embedded in the dense rings of Saturn cause density structures due to their gravitational interaction with the surrounding ring material which resemble a propeller, giving the structure its name in this way. The prediction of the existence of propeller structures within Saturn's rings [1, 2] led to their detection [3, 4, 5]. The recurrent observation of the large outer A ring propellers in Cassini ISS images allowed the reconstruction of their orbits. This analysis yielded that the observed propellers are deviating considerably from their expected Keplerian orbit [6]. The offset motion of the largest propeller structure called *Blériot* can be astonishingly well composed by a three-mode harmonic fit [7]. The origin of this offset motion still is on debate. Two hypotheses are in discussion: Whether the moonlet is perturbed resonantly by one or several of the large outer moons [7] or whether it is stochastically migrating [8, 9, 10]. Independent which of these hypotheses is finally correct, the changed orbital motion of the moonlet is effecting the shape of its created propeller structure. Here, we perform hydrodynamic simulations to study the changes of the propeller structure due to a disk-embedded moonlet which is librating around its mean orbital position. We present results showing how the induced propeller structure changes because of the libration of the moonlet and if these changes might be visible in Cassini images. Further, we apply our results to the propeller structures Blériot and Santos Dumont.

Acknowledgements

This work has been supported by the Deutsche Forschungsgemeinschaft (Sp 384/28-2, Ho 5720/1-1) and the Deutsches Zentrum für Luft- und Raumfahrt (OH 1401).

References

[1] Spahn, F., Sremčević, M., Density patterns induced by small moonlets in Saturn's rings?, Astronomy and Astrophysics , 358, 368–372, 2000.

[2] Sremčević, M. et al., Density structures in perturbed thin cold discs, Monthly Notices Royal Astron. Soc. , 337, 1139–1152, 2002.

[3] Tiscareno, M. S. et al., 100-metre-diameter moonlets in Saturn's A ring from observations of 'propeller' structures, Nature , 440, 648–650, 2006.

[4] Sremčević, M. et al., A belt of moonlets in Saturn's A ring, Nature , 449, 1019–1021, 2007.

[5] Tiscareno, M. S. et al., The Population of Propellers in Saturn's A Ring, Astronomical Journal , 135, 1083–1091, 2008.

[6] Tiscareno, M. S. et al., Physical Characteristics and Non-Keplerian Orbital Motion of 'Propeller' Moons Embedded in Saturn's Rings. Astrophysical Journal Letters , 718, L92–L96, 2010.

[7] Seiler, M. et al., A Librational Model for the Propeller Blériot in the Saturnian Ring System, Astrophysical Journal Letters 840, L16, 2017.

[8] Rein, H., Papaloizou, J. C. B., Stochastic orbital migration of small bodies in Saturn's rings, Astronomy and Astrophysics , 524, A22, 2010.

[9] Pan, M. et al., Stochastic flights of propellers, Monthly Notices Royal Astron. Soc. , 427, 2788–2796, 2012.

[10] Tiscareno, M. S., A modified "Type I migration" model for propeller moons in Saturn's rings, Planetary and Space Science 77, 136–142, 2013.

EPSC Abstracts
Vol. 12, EPSC2018-1198, 2018
European Planetary Science Congress 2018

Apse-alignement in narrow-eccentric ringlets. The comparative case of the ε-ring of Uranus and the ring system of (10199) Chariklo.

Mario Daniel Melita (1,2)

(1) Instituto de Astronomía y Física del Espacio (CONICET-UBA). CABA. Argentina (melita@iafe.uba.ar)

(2) Facultad de Astronomía y Geofísica. Universidad Nacional de La Plata, Argentina.

Abstract

The discovery of ring systems around objects of the outer Solar System provide a strong motivation to estimate better their physical and orbital properties, which shall help to refine models about their origin. In the case of the ring system of (10199) Chariklo, where there is evidence that the rings are eccentric, we apply a theory of apse-alignement, to derive information about the most plausible combinations of the values of its surface density, eccentricity and eccentricity-gradient, as well as the masses and location of their -presently undetected- shepherd-satellites.

1. Introduction

Ring systems have been recently discovered around the centaur (10199) Chariklo [1], trans-Neptunean object (136108) Haumea [2] and there is compelling evidence that (2060) Chiron [3] is also surrounded by rings. It has been shown that the rings of (10199) Chariklo are stable under close encounters with the major planets [4], but their migration timescale by Poynting-Robertson effect is approximately 10^7 yr [1] and the one by viscous collisional dissipation is only about 10^6 yr [1], which suggests that the rings are being confined in their present location by shepherd satellites, estimated to be of about 1km in size [1]. Moreover, occultations of (10199) Chariklo reveal that the rings are probably eccentric [5 and references therein]. We review the theoretical models of narrow-eccentric ringlets based on the equations of motion of the Lagrangian-displacement quantities, as it was applied to the ε-ring of Uranus and the Titan-ringlet of Saturn [6,7], and we apply it to the case of the ring system of (10199) Chariklo.

2. Methods

The angular momentum available to sustain the eccentric figure of the ring, which corresponds to the m=1 wave-mode, is supplied by the shepherd satellites and, for an outer Linblad resonance, is given by [6]:

$$(dJ_{m+1}/dt)/m+1=-(dE_{dis}/dt)/\Omega \quad (1)$$

where Ω is the orbital frequency, dJ_{m+1}/dt is the angular momentum time rate corresponding to the m+1 satellite gravitational perturbing potential and dE_{dis}/dt is the energy dissipation rate in the ring, which can be caused either by viscous self-interactions along the whole ring or by the extreme compaction that may occur at the pericenter. For the case of the ϵ-ring of Uranus, this condition gives an excellent agreement in the later case [6]. For Charilo's system we compute the favourable combinations of mass of the satellite and resonance wave number, m, such that condition (1) is satisfied, for the 2 mentioned models of dissipation.

On the other hand, the rigid precession condition can be put as,

$$(\Omega_0-\omega_{prec}(r_0)).e(r_0).r_0=g_{int}(r_0)/\Omega, \quad (2)$$

where Ω_0 is the pattern-frequency, $\omega_{prec}(a_0)$ is the local precession-frequency , r_0 is the distance to the central object, $e(r_0)$ the local eccentricity and $g_{int}(r_0)$ is the acceleration produced both by the self-gravity of the ring, gs_{SF}, and by self-

interations, g_{SI}. In the left-hand side we find the impulse necessary to kill the differential precession induced by the oblateness of the central object and on the right-hand side we find the forces that can counteract it. Using this condition, we can put a constraint on the value of the surface density and the collisional impulse [6]. This condition is obtained averaging in an angle that co-rotates with the pattern frequency, therefore we obtain a description radially across the ring.

3. Results

In Figure 1 we illustrate the radial distribution of impulses to produce a rigid precession. In Figure 2 we show the estimated mass of the shepherd satellite in the ring system of Chariklo, necessary to balance the eccentricity decay, calculated for 2 models of dissipation. In Figure 3 we plot the radially integrated self-interactions-impulse of each model.

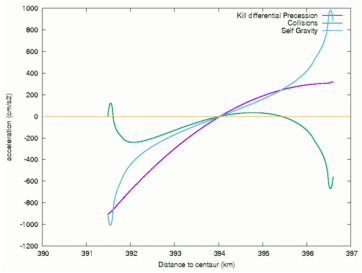

Figure 1: Radial distribution of impulses, $-g_{int}$, gs_{SF}, and g_{SI}. in Chariklo's system, for a model with eccentricity of 0.04, the eccentricity gradient 0.1 and surface density 20 g/cm^2.

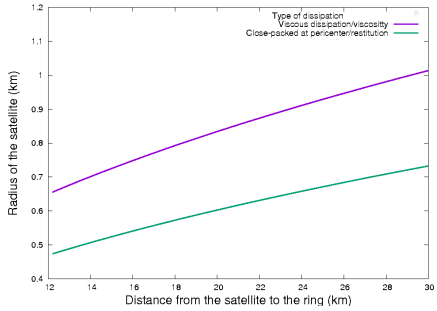

Figure 2: Estimated physical radii of the shepherd satellite (density 1g/cm^2), in Chariklo's system, as a function of the distance to the ring, for 2 models of dissipation. The eccentricity in this model is 0.012.

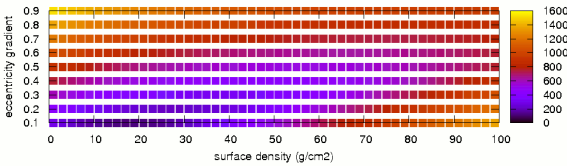

Figure 3: The integrated self-interactions impulse for different values of eccentricity gradient and surface density. The inner eccentricity in this case is 0.04.

4. Conclusions

We discuss how to produce a more precise determination of the mass of the ring system as well as the mass of the shepherds, for cases in which the rings are eccentric. When applied to the case of the centaur (10199) Chariklo we find that, if the ring is closed-packed at pericenter, the size of the shepherd satellites are in the range of ~1km. if not, their size can be considerably larger. Our preferred solution gives a plausible value for the surface density somewhat smaller than 20 g/cm^2 and a value eccentricity gradient of about 0.1. These results should offer additional constraints to primordial theories of these type of rings.

Acknowledgements

MDM acknowledges funding support for this project from ANPCyT PICT 1144/2013 and CONICET PIP 269/2015, Argentina.

References

[1] Braga-Ribas et al. 2014, Nature, 508, 72.
[2] Ortiz et al. 2017. Nature, 550, 219.
[3] Ortiz et al. 2015. A&A, 576. 12.
[4] Araujo, R. A. N., Sfair, R., & Winter, O. C. 2016, ApJ, 824, 80.
[5] Pan, M. & Wu, Y. 2016, ApJ, 821, 18.
[6] Papaloizou, J. C. B. & Melita, M. D. 2005, Icarus, 175, 435.
[7] Melita, M. D & Papaloizou, J. C. B. Cel.Mec.&Dyn.Ast. 2004. 19, 3.

EPSC Abstracts
Vol. 12, EPSC2018-1224, 2018
European Planetary Science Congress 2018

Modeling the size-distribution and granular velocity distribution in Saturn's rings

E.Seyfarth and F. Spahn, Institut für Physik und Astronomie, Universität Potsdam, Germany,
eseyfart@uni-potsdam.de

Abstract

1 Abstract

To understand the dynamics of Saturn's rings and its vertical structures at the B-ring-edge it is crucial to investigate the common evolution of the size- and granular velocity-distribution of the ring particles. Both distributions form a coupled dynamical system which we try to study in the following way:
First, for a given size-distribution we model the evolution of the velocity-distribution by assuming a Maxwellian including mass-dependend granular temperatures $T(m)$. A weighted average of the Boltzmann-equation yields expressions for the time derivative of the granular temperatures. The time-evolution of $T(m)$ is then dominated by collisional cooling (inelastic collisions) and viscous heating in the Keplerian shear. As an expression of the nonequilibrium, particles of different mass develop different granular temperatures (temperature-vector).
The development of the size-distribution can be obtained by a simulation of the particle-collisions using an erosive model in which every collision adds a distribution of smaller particles to the system and leaves a rest behind using collision parameters from [1] and [2]. The stationary size-distribution has the form of a power-law, assumed also in the former investigation of the velocity-distribution. In future we plan to derive a consistent coupled kinetic model of either distribution.

References

[1] Brilliantov, N.V., Albers, N. Spahn, F., Pöschel, T.: "Collision dynamics of granular particles with adhesion",Physical Review E: Statistical, Nonlinear, and Soft Matter Physics, Vol.76, 2007

[2] Bodrova, A., Schmidt, J., Spahn, F., Brilliantov, N.V.: "Adhesion and collisional release of particles in dense planetary rings", Icarus, Vol. 218, Issue 1, 2012

EPSC Abstracts
Vol. 12, EPSC2018-1225, 2018
European Planetary Science Congress 2018

The dust environment of Saturn within Saturn's D ring: CDA results of the Grand Finale of Cassini

Ralf Srama (1), Sean Hsu (2), Sascha Kempf (2), Georg Moragas-Klostermeyer (1), Mihaly Horanyi (2), Frank Postberg (3), Nozair Khawaja (3), Jonas Simolka (1), Nicolas Altobelli (4), Thomas Albin (1), Frank Spahn (5), Martin Seiss (5)

(1) Institute for Space Systems, University Stuttgart, Ger, (srama@irs.uni-stuttgart.de)
(2) University of Colorado, LASP, Boulder, USA
(3) University Heidelberg, Ger
(4) ESA-ESAC, Madrid, ESP
(5) University of Potsdam, Ger

Abstract

The Grand Finale of the Cassini spacecraft with its unique proximal orbits allowed fantastic scientific discoveries between April and September 2017. Cassini crossed the ring plane 22 times at a distance which was so close, that it touched the clouds of Saturn. The Cosmic Dust Analyzer observed unexpected high densities of tiny dust grains. On the other hand, larger grains above one micrometer were found to be highly depleted. The mass distribution of the grains detected peaks well below 70 nm and is cut off by the calibrated mass threshold. The dust density varied along the trajectory with overall consistent results during different ring plane crossings. Significant number of particles were detected above the ring plane, in the ring plane and below the ring plane at latitudes between +/-45 degrees. The measured density profiles are compared with latest models of nanograins ejected by the B and C ring. This paper summarizes the current understanding of this "Ring Rain", starting at Saturn's main ring and ending in Saturn's atmosphere. Density profiles, mass distributions and early compositional variations are reported.

Acknowledgements

The DDA investigation is supported under the DLR grant 50OH1501.

EPSC Abstracts
Vol. 12, EPSC2018-1266, 2018
European Planetary Science Congress 2018

Behaviour of a stochastic parametric oscillator with application to dust particles originating in the inner Saturnian rings

D. Schirdewahn, F. Spahn
University of Potsdam, Germany (dschirde@uni-potsdam.de)

Abstract

The differential equation of a harmonic oscillator

$$\ddot{x} + \omega^2 x = 0 \tag{1}$$

naturally arises when linearising non-linear dynamical equations. Such oscillators easily become a stochastic problem, if the coefficient ω^2 depends on system parameters that are subject to random changes.
Assuming a parametric noise

$$\omega^2 = \omega_0^2(1 + \xi(t)) \tag{2}$$

we examine cases for both continuous and discrete stochastic processes $\xi(t)$ and find expressions for the Lyapunov Exponent

$$\lambda := \lim_{t\to\infty} \frac{1}{2t} \overline{\log E} \tag{3}$$

[1][2], with the energy-like expression

$$E(t) = \frac{1}{2}x^2(t) + \frac{1}{2}\dot{x}^2(t) \quad . \tag{4}$$

The Lyapunov exponent, which is the time-averaged exponential growth rate of $E(t)$, permits to distinguish between growing and decaying branches of the solution $x(t)$.

These results, together with general stability considerations are applied to charged dust particles, that are eroded in the inner rings of Saturn - for example as ejecta from impacts of interplanetary micrometeoroids. The charge q of those particles might change erratically due to varying charging fluxes or impacts/losses of single charge carriers. The first description is suitable for large particles that carry several additional charges, the second one for small particles, where single charging events have to be taken into account. These events are assumed to be poissonian distributed [3].

After an identification of the values of critical influences - i.e. the charging fluxes and the equilibrium charge, we compare the time scales of charging, stochastic growth (given by $1/\lambda$), and periodic motion of the epicyclically approximated particle motion.
This comparison finally allows to decide, for which particle sizes and initial positions in the rings, erratic motion due to charge fluctuations becomes important.

Acknowledgements

This work is partially supported by the Deutsche Forschungsgemeinschaft (Sp384/33-1).

References

[1] Mallick, K., Peyneau P.-E.: Phase diagram of the random frequency oscillator: The case of Ornstein–Uhlenbeck noise, Physica D: Nonlinear Phenomena, Vol. 221 (1), pp. 72-83, 2006.

[2] Mallick, K., Marcq, P.: Stability analysis of a noise-induced Hopf bifurcation, Eur. Phys. J. B, Vol 36 (1), pp. 119-128, 2003

[3] Hsu, H.-W., Postberg, F., Kempf, S., Trieloff, M., Burton, M., Roy, M., Moragas-Klostermeyer, G., Srama, R.: Stream particles as the probe of the dust-plasma-magnetosphere interaction at Saturn, J. Geophys. Res., Vol. 116, A09215, 2001

EPSC Abstracts
Vol. 12, EPSC2018-1277, 2018
European Planetary Science Congress 2018

What confines the rings of Saturn?

Radwan Tajeddine (1), Philip D. Nicholson (2), Pierre-Yves Longaretti (3,4), Maryame El Moutamid (1), Joseph A. Burns (5)

(1) Center for Astrophysics and Planetary Science, Cornell University, Ithaca, NY 14853, USA (tajeddine@astro.cornell.edu)
(2) Department of Astronomy, Cornell University, Ithaca, NY 14853, USA
(3) Université Grenoble Alpes (UGA), France
(4) CNRS/INSU – Institut de Planétologie et d'Astrophysique de Grenoble (IPAG), UMR 5274, France
(5) College of Engineering, Cornell University, Ithaca, NY 14853, USA

Abstract

The viscous spreading of planetary rings is believed to be counteracted by satellite torques, either through an individual resonance or through overlapping resonances (when the satellite is close to the ring edge). For the A ring of Saturn, it has been commonly believed that the satellite Janus alone can prevent the ring from spreading via its 7:6 Lindblad resonance. We discuss this common misconception and show that, in reality, the A ring is confined by the contributions from the group of satellites Pan, Atlas, Prometheus, Pandora, Janus, Epimetheus, and Mimas, whose resonances gradually decrease the angular momentum flux (AMF) transported outward through the ring via density and bending waves. We further argue that this decrease in angular momentum flux occurs through the mechanism of 'flux reversal'.

Furthermore, we use the magnitude of the satellites' resonance torques to estimate the effective viscosity profile across the A ring, showing that it decreases from ~50 $cm^2 s^{-1}$ at the inner edge to less than ~11 $cm^2 s^{-1}$ at the outer edge. The gradual estimated decrease of the angular momentum flux and effective viscosity are roughly consistent with results obtained by balancing the shepherding torques from Pan and Daphnis with the viscous torque at the edges of the Encke and Keeler gaps, as well as the edge of the A ring.

1. Introduction

The confinement of the rings of Saturn was for a long time an unsolved matter. The satellite Atlas might be expected to play a major role in confining the A ring through the shepherding mechanism since it is the closest satellite to its outer edge. However, Voyager imaging and occultation data showed that the edge of the A ring appears to be in a 7:6 Inner Lindblad Resonance (ILR) with the more massive satellite Janus [1]. Thus, it has been generally believed that the torque exerted by this resonance confines the entire A ring. On the other hand, the B ring's outer edge has been clearly shown to be controlled by the 2:1 ILR with Mimas [1, 2, 3]. This resonance, the strongest anywhere in Saturn's rings, is believed to prevent the B ring from spreading outwards and also to be responsible indirectly for the existence of the Cassini division [4].

In this work, we study the effect of resonance torques due to multiple satellites on the confinement of the A and B rings of Saturn, as well as on the orbital evolution of the satellites. We also estimate the viscosity in the A and B rings by balancing satellite and ring torques. See [5] for more details.

2. Satellite resonance torques

At a Lindblad (Vertical) resonance, perturbations from the satellite excite the ring particles' eccentricities (inclinations). As the ring particles oscillate radially (vertically), their perturbations are transferred via self-gravity to the neighboring ring particles closer to the satellite and farther from the resonance location. As a result, a trailing spiral density wave is created, which propagates radially towards (away from) the perturbing satellite across the ring for a Lindblad (Vertical) resonance. Subsequently, the density wave is damped by collisions between the ring particles as it propagates through the ring causing these particles to lose (for a satellite outside the rings) or gain (for a satellite inside the rings) angular momentum and drift back towards the resonant location.

If the resonant torque from a satellite's Inner Lindblad Resonance (ILR) is stronger than the local viscous torque in the ring, we expect that a gap with a sharp inner edge should open at the resonance

location. However, even if the resonant torque is smaller and no gap forms, then the satellite resonance will still exert a negative torque on the ring, via a density wave, which will reduce the outward flux of angular momentum through the rings. In this scenario, the Janus 7:6 ILR is responsible only for removing the flux that has 'survived' all of the previous similar satellite resonances. To quantify this picture, we calculate the variation of the AMF across the A ring taking into account *all* of the first and second order Lindblad resonances due to the satellites Pan, Atlas, Prometheus, Pandora, Janus, Epimetheus, and Mimas, as well as the strongest (i.e., second-order) vertical resonances due to Mimas, counting a total of 397 satellite resonances present in the A ring.

Figure 1 shows the resulting upper and lower limits on the AMF and the inferred viscosity as a function of radius across the A ring. As might be expected, this plot shows a gradual outward decrease in the AMF (Fig. 1a) through the ring as we encounter successive resonances with the external satellites. On the other hand, calculations of satellite resonance torques on the B ring show that the Mimas 2:1 ILR alone can confine this ring.

3. Discussion and Conclusion

A careful accounting of all known satellite resonances in the A and B rings reveals that, in the A ring, the radial confinement of the ring against viscous spreading is distributed over many resonances. As a result, the AMF is expected to decrease outwards across the ring. For the B ring, on the other hand, almost all of the work is done by the Mimas 2:1 ILR located at the outer edge. By equating the computed AMF with that expected to be transported by collisional interactions within the rings, we derive a radial profile of transport viscosity across both rings. In the A ring this is found to be roughly consistent with viscosities inferred from torque balancing at the Encke and Keeler gaps, but no such direct test is possible for the B ring. We speculate that the observed steep decrease in AMF in the trans-Encke region of the A ring may be due to "flux reversal" associated with the disturbed streamlines produced by the large concentration of density waves driven by satellite resonances in this region, which translates into a decrease in effective viscosity.

a

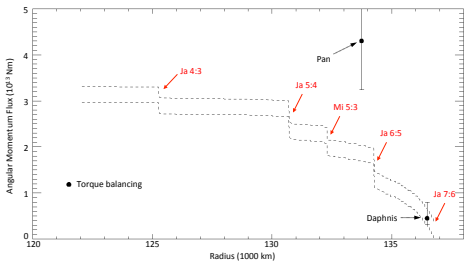

b

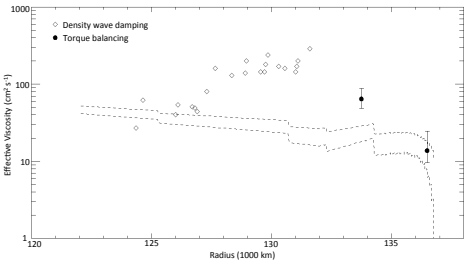

Figure 1: Upper and lower limit estimates (dashed lines) of (a) the AMF and (b) the effective viscosity (on a log scale) in the A ring as a function of radius, taking into account all the first and second order Lindblad resonances from the satellites and the 5:3 bending wave from Mimas.

Acknowledgements

We gratefully thank Peter Goldreich for a brief but valuable discussion on this topic.

References

[1] Porco C.C. et al., Saturn's nonaxisymmetric ring edges at 1.95 R(s) and 2.27 R(s), *Icarus*, **60**, 17-28 (1984).

[2] Spitale J.N. and Porco C.C., Detection of Free Unstable Modes and Massive Bodies in Saturn's Outer B Ring, *Astron. J.*, **140** (6), 1747-1757 (2010).

[3] Nicholson P.D. et al. Noncircular features in Saturn's rings I: The edge of the B ring, *Icarus*, **227**, 152-175 (2014).

[4] Goldreich P. and Tremaine S.D., The formation of the Cassini division in Saturn's rings, *Icarus*, **34**, 240-253 (1978a).

[5] Tajeddine et al., What confines the rings of Saturn, *Astrophys. J. Supp.*, **232**, 28 (2017).